J. Membrane Biol. 187, 213–223 (2002)
DOI: 10.1007/s00232-001-0165-3

The Journal of
Membrane
Biology

Temperature Dependence of Bistability in Squid Giant Axons with Alkaline Intracellular pH

J.R. Clay[1], **A. Shrier**[2]
[1]Ion Channel Biophysics Unit, Division of Intramural Research, National Institute of Neurological Disorders and Stroke, National Institutes of Health, Bethesda, MD 20892 USA
[2]Department of Physiology, McGill University, Montreal, Quebec, Canada H3G 1Y6

Received: 30 October 2001/Revised: 28 February 2002

Abstract. Raising the intracellular pH (pH_i) above 7.7 in intracellularly perfused squid giant axons causes spontaneous firing of action potentials. The firing frequency ranged from 20 Hz at 0°C to 200 Hz at 23°C. Above 23°C, the axons were quiescent. They were bistable for $13 < T < 23$°C. That is, they were either quiescent or spontaneously firing. Below 13°C, spontaneous firing was the only stable element. The primary effects of changes in temperature on the underlying ionic currents were on gating of the delayed rectifier potassium channel I_K, and the sodium ion channel I_{Na}. The kinetics of I_K had a Q_{10} of 3.63. The effect of T on I_{Na} was more complicated in that the peak I_{Na} amplitude increased with T, as demonstrated in earlier reports. This effect, as well as the changes in I_{Na} kinetics produced by changes in T, were mimicked in the context of a model of I_{Na} gating in which activation and inactivations are coupled. Electrical activity was simulated in a model of the action potential with appropriate temperature-dependent modifications for I_{Na} and I_K. The model predicts a change from monostability (spontaneous firing) at relatively low temperatures to bistability (quiescence and spontaneous firing) as the temperature is raised, followed by change back to monostability (quiescence) as the temperature is further increased, which is consistent with the experimental results.

Key words: Nerve — Automaticity — Alkalinity — Action potential — Temperature — Ion channel gating

Correspondence to: J.R. Clay; email: jrclay@ninds.nih.gov

Introduction

Excitable membranes usually exhibit a single type of behavior in response to a given set of experimental conditions. For example, axons either rest quiescently in the absence of a stimulus, or they generate an action potential in response to a depolarizing current pulse of sufficiently large amplitude (Hodgkin & Huxley, 1952). In a few instances two qualitatively different types of behavior for one set of conditions have been observed, such as repetitive firing and quiescence. This form of bistability occurs in squid giant axons with reduced external calcium ion concentration (Guttman, Lewis & Rinzel, 1980) and in pacemaker cardiac cells (Jalife & Antzelevitch, 1979; Shrier, Clay & Brochu, 1990). Transitions between the two stable states—quiescence and repetitive firing—can be produced with current pulses. For example, a brief-duration depolarizing pulse can shift these preparations from quiescence to repetitive firing and, conversely, an appropriately timed current pulse can annihilate repetitive firing, thereby shifting the preparations to their resting state (Jalife and Antzelevitch, 1979, Guttman et al., 1980;).

Even though a repetitive train of action potentials (APs) can be elicited from squid giant axons with a sustained depolarizing current pulse in seawater containing reduced calcium ion concentration (Guttman, et al., 1980), similar behavior has not been observed under physiological conditions (Clay, 1998). Only a single AP is elicited, regardless of pulse amplitude or duration, which is consistent with the role the axon plays in squid behavior (Otis and Gilly, 1990; Clay, 1998). Recently, we discovered, serendipitously, that the axon fires APs repetitively in the absence of current pulses, i.e., it becomes an autonomous oscillator, when the intracellular pH (pH_i) is made slightly alkaline—7.7 or higher (Clay & Shrier, 2001). Normal pH_i is 7.3. Those experiments were

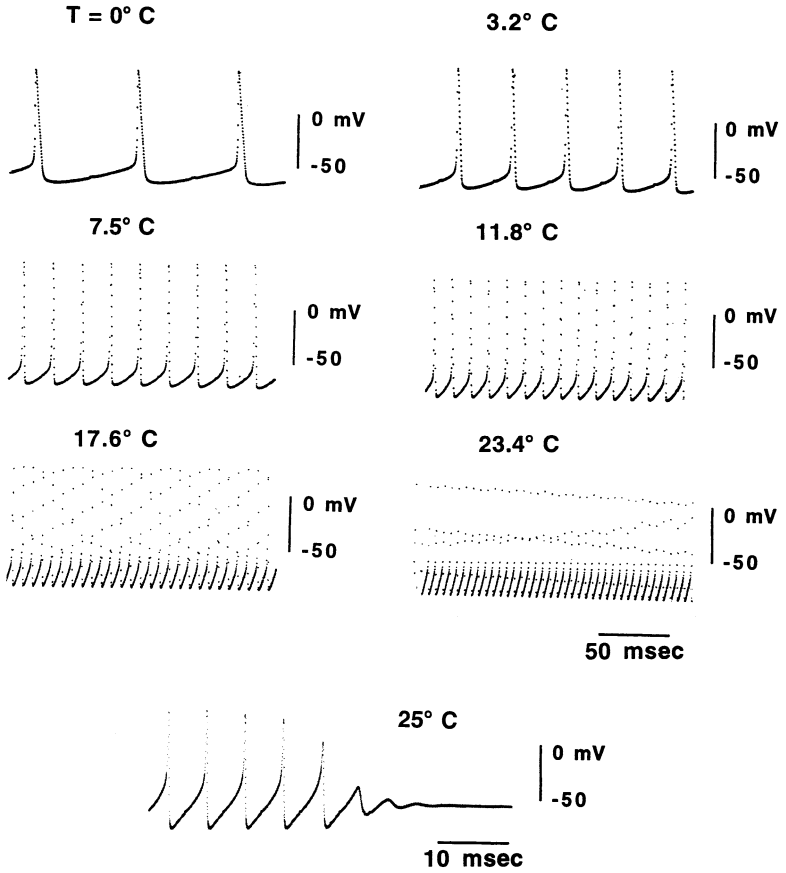

Fig. 1. Temperature dependence of spontaneous firing in squid axons with elevated pH_i (pH = 8.5). Bottom panel: Shortly after increasing T to 25°C, the axon ceased firing. The final few APs prior to cessation of activity are shown here.

carried out at relatively low temperatures ($T \sim 5$°C). As shown in this report, the axon is bistable with alkaline pH_i when the temperature is within the physiological range of the animal ($T \sim 15$°C). These results have been simulated using the Clay (1998) model of squid giant axon electrical activity by adding the appropriate temperature dependence to the gating parameters of the sodium and potassium ion currents. As noted in our recent report (Clay & Shrier, 2001), this preparation may serve as a useful model for questions of rhythmicity in nerve cell preparations, given the robustness of these results.

Materials and Methods

Experiments were performed on giant axons from the common North Atlantic squid (*Loligo pealei*) at the Marine Biological Laboratory in Woods Hole, MA, using the axial wire voltage- and current-clamp technique with intracellular perfusion, as described in Clay and Shlesinger (1983). The temperature in these preparations ranged between 0°C and 30°C. In any given experiment it was maintained constant to within 0.1°C by a negative feedback circuit connected to a Peltier device located within the experimental chamber. The external solution was artificial seawater, which consisted (in mM) of 430 NaCl, 10 KCl, 10 $CaCl_2$, 50 $MgCl_2$, and 10 Tris-HCl (pH = 7.5). The intracellular solution consisted (in mM) of 400 sucrose, 250 KF, 30 Na glutamate, and 50 K glutamate, with the pH titrated to 8.5 by free glutamic acid. For these conditions, the reversal potential for potassium ions, E_K, was −80 mV and E_{Na}, the sodium ion reversal potential, was 64 mV. The voltage-clamp recordings of the delayed rectifier potassium ion current I_K in Fig. 8 were obtained with tetrodotoxin (TTX, Sigma) added to the external solution to block the sodium ion current, I_{Na}. The recordings of I_{Na} in Fig. 9 were obtained with an intracellular perfusate that consisted of 400 mM sucrose, 250 mM CsF, and 50 mM Na glutamate (pH 7.2). This perfusate effectively eliminates I_K.

Computer simulations were carried out with the Mathematica software package (Wolfram, 1999) using the revised model of the squid giant axon action potential previously described (Clay, 1998; Clay & Shrier, 2001). The equations for the ionic current components are given below (*see* Appendix).

Results

Spontaneous Firing of Action Potentials with Alkaline pH_i—Temperature Dependence

Squid giant axons are transformed into autonomous oscillators when the intracellular pH (pH_i) is raised above ~7.7 (Clay & Shrier, 2001). The temperature dependence of the activity is illustrated in Fig. 1. The firing frequency at 0°C in this preparation was 13 Hz, which was increased to 27, 50, 79, 143, and 242 Hz as the temperature was raised to 3.2, 7.5, 11.8, 17.6, and 23.4°C, respectively. At higher temperatures the axon was not spontaneously active. For example, activity ceased in the experiment illustrated in Fig. 1 shortly

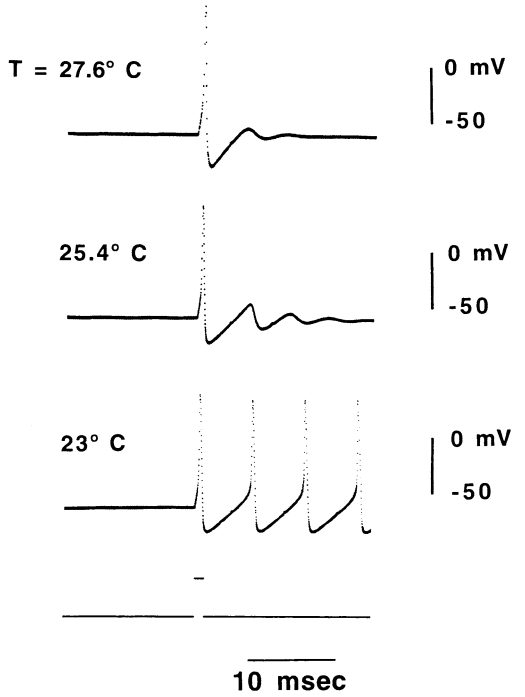

Fig. 2. Transition from bistability to quiescence for $T > 23$°C. Same preparation as in Fig. 1. Above $T = 23$°C, an action potential was elicited by a current pulse (top two panels). The current pulse for all 3 results is shown in the bottom panel. When T was reduced from 27.6° to 25.4°C, oscillations ("ringing") of the membrane potential occurred following the AP. At 23°C, spontaneous activity was re-established.

after the temperature was raised to 25°C. The final few APs prior to cessation of activity are shown here (bottom panel, Fig. 1). Brief-duration current pulses elicited APs for $T = 27.6$°C (Fig. 2, top panel). When the temperature was reduced to 25.4°C, the membrane potential oscillated significantly following the AP (Fig. 2, middle panel). At 23°C, spontaneous activity was re-established with a current pulse (Fig. 2, bottom panel). In other words, the axon was monostable for $T > 23$°, with the resting potential as the only stable element. Below 23°C the axon was bistable. Bistability was observed for $13 < T < 23$° (Fig. 3). Pooled results from four different axons, which illustrate this result as well as the temperature dependence of the frequency of spontaneous firing, are given in Fig. 3. All of these results were obtained with $pH_i = 8.5$. As noted previously (Clay & Shrier, 2001), both the firing frequency and the shape of the voltage waveform during the activity were independent of pH_i in the 7.7 to 8.5 range.

As indicated in Fig. 3, spontaneous activity was the only stable feature observed in these preparations for $T < 13$°C. A result in support of this conclusion is illustrated in Fig. 4. As noted by Winfree (1977), a brief-duration current pulse of the appropriate amplitude that impinges upon a neural pacemaker can either annihilate the repetitive activity or cause an abrupt discontinuity in the phase of the action potential train when the pulse is applied at a critical point in the pacemaker cycle. The former case corresponds to bistability, the latter to monostability, i.e., spontaneous firing continues following a pulse, regardless of pulse amplitude or duration. In the experiment described in Fig. 4, a 1-msec pulse of fixed amplitude was applied at a given time, T_p, in the unperturbed cycle, one pulse every 10 APs ($T = 5$°C), and T_p was advanced in 1-msec increments. At early times in the cycle relatively little change occurred in the time T_1 of the AP subsequent to the pulse (top panel, Fig. 4*A*). In other words, the phase of the repetitive activity was essentially unchanged. At a critical point ($T_p/T_0 \sim 0.6$, where T_0 is the duration of the unperturbed cycle), a significant increase in T_1

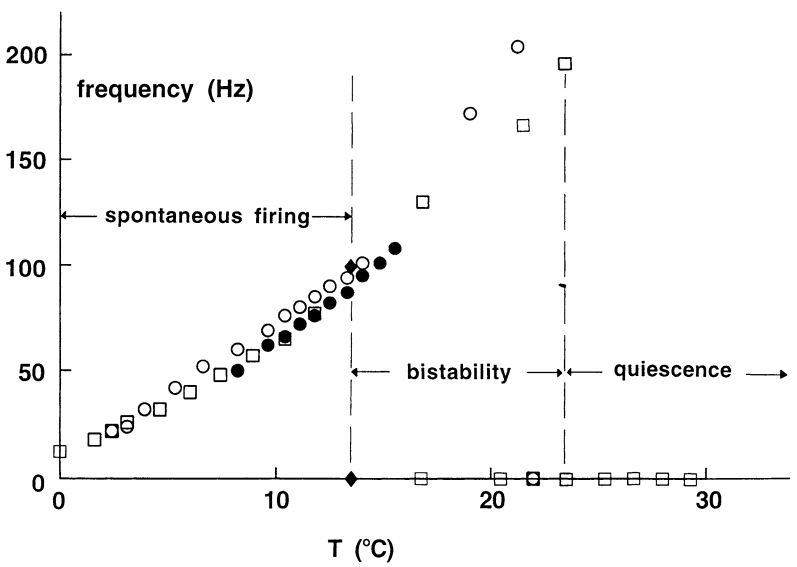

Fig. 3. Frequency of firing *vs.* temperature. Each symbol represents a different preparation. Below 13°C, only spontaneous firing was observed. Bistability was observed for $13 < T < 23$°C. Above 23°C, the axons were quiescent.

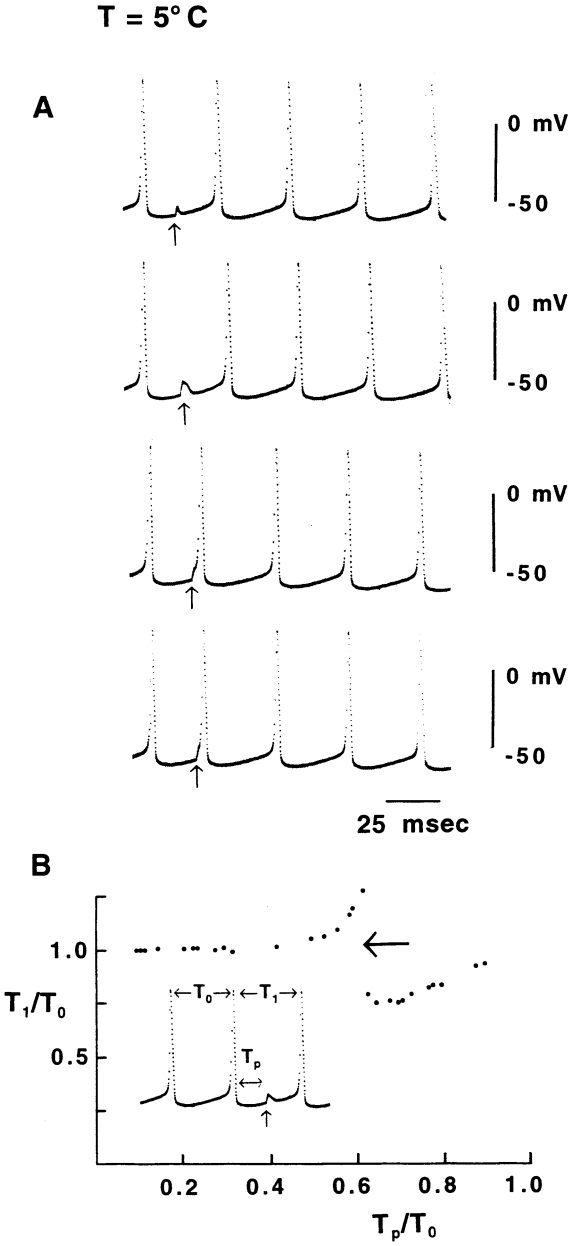

Fig. 4. Phase resetting of spontaneous firing at $T = 5$°C. (*A*) A 1-msec depolarizing current pulse was applied at the time (T_p) indicated by the arrow below each recording. (*B*) The time of the AP subsequent to the pulse (T_1) is plotted as a function of T_p (with both T_1 and T_p normalized to the length of the unperturbed cycle, T_0). At $T_p/T_0 \sim 0.6$, an abrupt transition in phase resetting occurred (*middle* two panels of *A*) as predicted by Winfree (1977) for a preparation without stable resting state. That is, the activity could not be annihilated by current pulses.

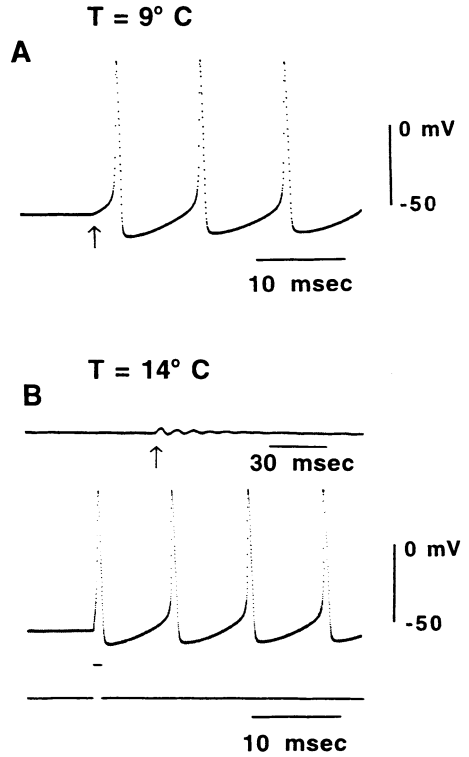

Fig. 5. Temperature-dependent transition from monostability (spontaneous firing) to bistability (spontaneous firing plus a coexisting, stable resting state). (*A*) A spontaneously firing axon ($T = 9$°C) was held in voltage clamp at −60 mV. Upon release of the clamp (arrow below the recording) spontaneous firing immediately recommenced. (*B*) The temperature was increased to 14°C. Same preparation as in (*A*). Spontaneous firing continued at a slightly higher rate than at 9°C (*not shown*). The axon was once again clamped at −60 mV (*top panel*). Upon release of the clamp (indicated by the arrow) the membrane potential oscillated slightly as it relaxed to a stable rest potential (−57 mV). Spontaneous firing was re-established by a brief-duration current pulse (*bottom panel*, *B*).

occurred. When the pulse was applied 1 msec later, the phase was abruptly advanced (third panel, Fig 4*A*). An AP was elicited almost immediately. A similar result occurred for all later times in the cycle (bottom panel, Fig. 4*A*). This discontinuity in phase resetting is illustrated by the arrow in Fig. 4*B*. The activity was not annihilated regardless of pulse amplitude (other results not shown) in contrast to Guttman et al. (1980), who were able to terminate repetitive firing in squid giant axons exposed to low Ca^{2+} seawater with brief-duration current pulses.

Monostability (spontaneous firing without a coexisting, stable rest state) was also demonstrated using voltage clamp (Fig. 5). Spontaneous firing was abolished by clamping the axons at −60 mV. Monostable preparations began firing immediately after the clamp was released, as illustrated by the experiment in Fig. 5*A* ($T = 9$°C). When the temperature was increased to 14°C, the axon continued to fire spontaneously (*not shown*). The activity was abolished by clamping the axon at −60 mV. This time, the axon was quiescent after the clamp was released (arrow in Fig. 4B, top panel). A small oscillation occurred as the membrane potential relaxed to its resting level (−57 mV). Spontaneous firing was re-established with a brief-duration current pulse (Fig. 5*B*, bottom panel).

In other words, axons with elevated pH_i, exhibited a second temperature-dependent transition from monostability to bistability—a different transition from that illustrated in Fig. 2, in that the monostable element for $T < 13$°C was spontaneous firing.

Ionic Mechanism of Spontaneous Firing

We previously modeled the spontaneous activity observed in squid giant axons with alkaline pH_i by assuming that the "leak" current, I_L, was essentially eliminated under these conditions, i.e., I_L is activated by intracellular protons (Clay & Shrier, 2001). The model also contained, in addition to I_K and I_{Na}, a persistent sodium ion current, I_{NaP}, and an inward rectifier potassium ion current, $I_{K,ir}$ (Clay & Shrier, 2001). The latter was found necessary in order to simulate our results. However, experimental evidence for $I_{K,ir}$ is lacking in squid giant axons. We previously failed to include in our model the Cl^- conductance (Inoue, 1985). Replacing $I_{K,ir}$ with I_{Cl} brings the model more in line with voltage-clamp measurements of ionic currents, and is sufficient to mimic spontaneous firing, as in our previous model, by retaining the assumption that the only change with alkaline pH_i is the removal of I_L. The steady-state current-voltage relation with I_L ($pH_i = 7.3$) and without I_L ($pH_i = 8.5$) is shown in Fig. 6*A*. The membrane potential at which this relation crosses the voltage axis is referred to as V_0. With $pH_i = 7.3$, $V_0 = -55$ mV. With $pH_i = 8.5$, $V_0 = -57$ mV. That is, V_0 is hyperpolarized following removal of I_L, as is to be expected with a net loss of inward current, given that the reversal potential for I_L is -49 mV (*see* Appendix). The current-voltage relation with $I_L = 0$ also has a negative slope character for $V < -63$ mV, which is attributable to I_{NaP}. With $pH_i = 7.3$, V_0 is stable. A brief-duration current pulse elicits an AP followed by a return of the membrane potential to V_0 (Fig. 6*B*). With $pH_i = 8.5$, V_0 is unstable. When the model is set at steady-state conditions in the vicinity of V_0, the membrane potential begins to oscillate. The oscillations grow in amplitude until an unending train of APs occurs (Fig. 6*C*). This result is counterintuitive given that the spontaneous firing is produced by a net loss of inward current in the subthreshold potential range. The mechanism is, in part, the negative slope character of I_{NaP}, which is masked by I_L with $pH_i = 7.3$. When I_L is removed, I_{NaP} together with I_K and I_{Na} destabilizes the resting state even though the slope of the steady-state current-voltage relation at V_0 is positive. The impedance—the inverse of the slope conductance at V_0—is significantly increased, so that small changes in net membrane current will produce a larger change in membrane potential than at $pH_i = 7.3$, changes which, together with the I_{Na} and I_K kinetics, ultimately cause V to cross threshold of the AP.

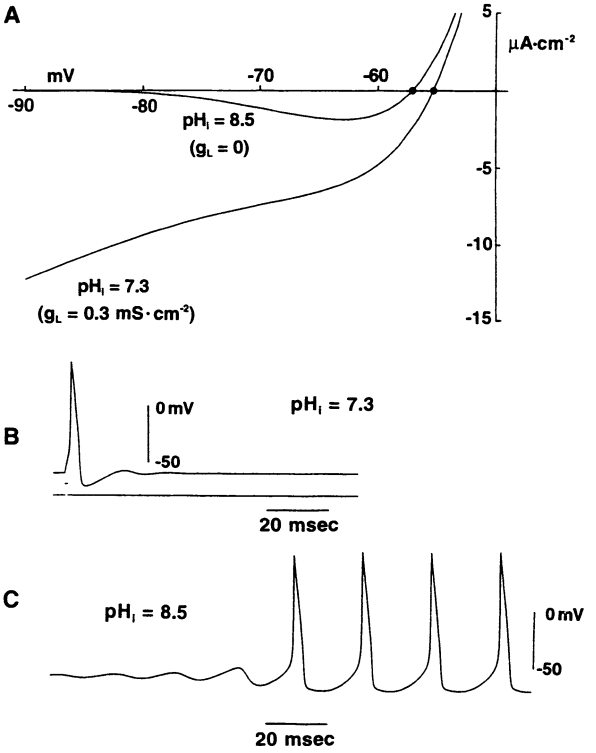

Fig. 6. (*A*) Steady-state current-voltage relations of the ionic model described in the text for $pH_i = 7.3$ and 8.5. The sole difference between the two conditions in the model is the absence of I_L for $pH_i = 8.5$. The potential at which each curve crossed the voltage axis, V_0, is represented by the symbol (•). With $pH_i = 7.3$, V_0 is stable (rest potential), whereas with $pH_i = 8.5$, V_0 was unstable, as described in the text. (*B*) Electrical activity for the two conditions. A current pulse elicited an AP with $pH_i = 7.3$, followed by return of the membrane potential to rest. A stimulus was not required to produce electrical activity with $pH_i = 8.5$. The membrane potential moved away from V_0 in an oscillatory manner until AP threshold was crossed, resulting in an unending train of Aps.

The results in Fig. 6*B* and *C* are plotted in a different manner in Fig. 7*A* and *B*, respectively. The net current, $I_K + I_{Na} + I_{Cl} + I_L + I_{NaP} + I_{stim}$, where I_{stim} is the stimulus in Fig. 6*B*, is plotted *vs.* membrane potential, with time t as an implicit parameter. (The direction of time is indicated by the arrows in Fig. 7). The action potential in Fig. 6*B* ($pH_i = 7.3$) traverses a trajectory (Fig. 7*A*) in current-voltage space before returning to the resting potential, V_0 (inset of Fig. 7*A*). With $pH_i = 8.5$, the trajectory spirals away from V_0 and ultimately traverses the action potential cycle repeatedly during the unending AP train, in what is termed a limit cycle oscillation (Winfree, 1977).

Temperature Dependence of Ionic Currents

The primary effect of temperature on membrane currents in squid axons is on I_K and I_{Na} gating. The

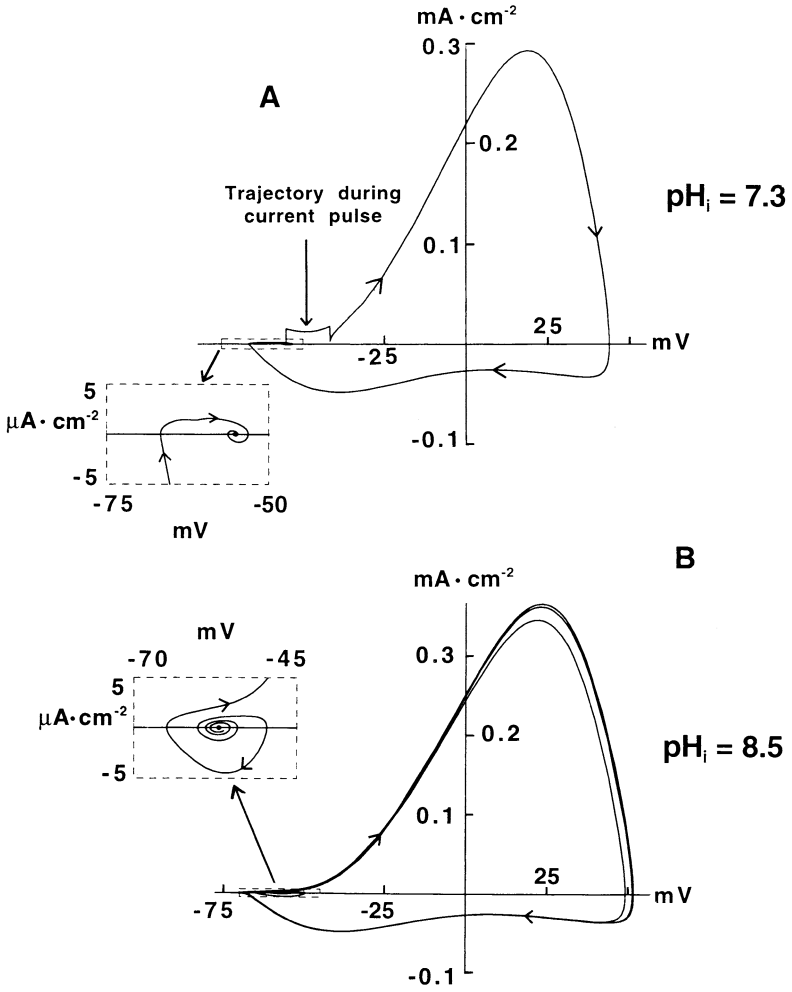

Fig. 7. Current-voltage plots of the activity illustrated in Fig. 6*B*. (*A*) Trajectory of membrane potential *vs.* membrane current at $pH_i = 7.3$. The loop corresponds to the AP with time t as a parameter. The direction of time is indicated by the arrows. Following the AP, the system returned to rest in a spiral manner as indicated by the inset. (*B*) Similar plot as in *A* for $pH_i = 8.5$. The membrane potential spiraled away from V_0 when the model was initialized close to this potential. It ultimately traversed the AP trajectory repeatedly in what is referred to as a limit cycle oscillation (Winfree, 1977). That is, V_0 is the only stable element for $pH_i = 7.3$, whereas the limit cycle is the only stable element for $pH_i = 8.5$ ($T = 5$°C).

time-independent background current, i.e., $I_{Cl} + I_{NaP} + I_L$, appears to have a relatively small temperature dependence.

An increase in temperature speeds I_K kinetics (Fig. 8). These recordings were obtained with TTX (1 μM) and a voltage step to +20 mV (holding potential −80 mV). They are shown superimposed with a fit (indistinguishable from the data) of $[1-\exp(-t/\tau)]^6$ with a plot of τ *vs.* T below the recordings. The Q_{10} was 3.63, as compared to $Q_{10} = 3$ in the Hodgkin and Huxley (1952) model. Frankenhauser and Moore (1963) reported a similar result for the Q_{10} of I_K in myelinated axons.

Recordings of I_{Na} at various different temperatures are illustrated in Fig. 9. As with I_K, the I_{Na} kinetics increase with increasing T. In addition, the peak I_{Na} current amplitude was temperature dependent, as originally reported in frog and rabbit myelinated axons by Chiu, Mrose, and Ritchie (1979) and in squid giant axons by Kimura and Meves (1979) and Matteson and Armstrong (1982). We have described these results using the Vandenberg and Bezanilla (1991) model of I_{Na} gating which is given by:

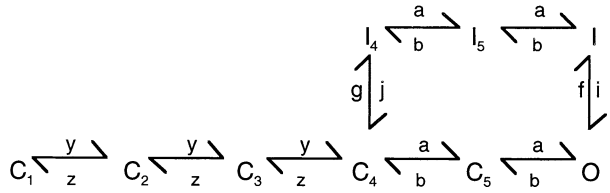

where C_i ($i = 1,2...5$) are closed states, I_4, I_5, and I are inactivated states, and O is the open (conducting) state of the channel. The various voltage-dependent rate parameters of the model, $a, b, c, d, g, j, f, l, y$, and z, are given in the Appendix. All of these parameters are assumed to have a temperature dependence (*see* Appendix) except for g and j, the rate constants connecting C_4 and I_4. Specifically, a, b, y, and z were all assumed to have the same temperature-dependent factor, $fact_a$, whereas f and i were assumed to have a different temperature-dependent factor, $fact_i$. These parameters were adjusted so as to give a reasonable fit, by eye, to the experimental records for $V = -20$ mV. The results for $fact_a$ and $fact_i$ along with the corresponding simulations of I_{Na} from the Vandenberg and Bezanilla (1991) model are shown in Fig. 10. The $fact_a$

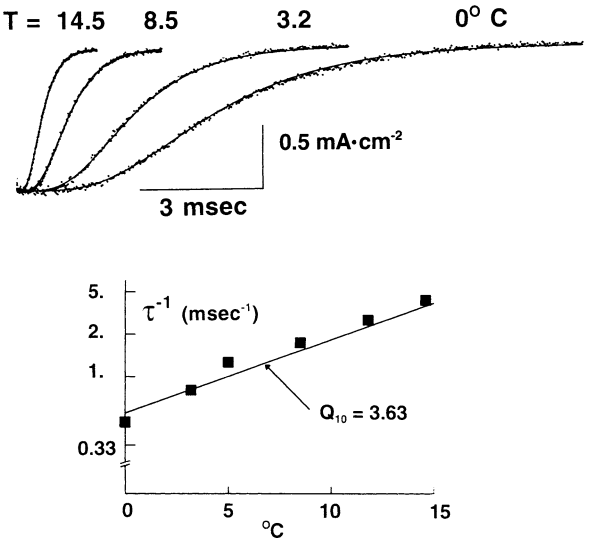

Fig. 8. Temperature dependence of I_K. The recordings in the upper left were obtained from an axon with TTX added to the external medium to block I_{Na} with voltage steps to +20 mV (holding potential −80mV). The results from four different temperatures are shown superimposed. Each record was fit (by eye) with $[1-\exp(-t/\tau)]^6$. The fits are virtually indistinguishable from the data. A plot of τ *vs.* T is shown below the recordings. The line is a best fit of the points having a Q_{10} of 3.63.

results have a Q_{10} of 2.5. The $fact_i$ results appear to saturate above 10°C. They were described by $2[(3^{(T-5)/10})/(1+3^{(T-5)/10})]$. A similar biphasic dependence of inactivation gating on T was originally reported for rabbit myelinated axons by Chiu et al. (1979). Clearly, other mechanisms may describe the results in Fig. 10 equally well. Our primary purpose was to have a theoretical model of the temperature dependence of I_{Na} for our simulations of membrane excitability.

Simulations of the Effect of Temperature on Electrical Activity

As noted above, our model does not have a stable resting state with $I_L = 0$ for relatively low temperatures ($T \sim 5$°C), which is true also for the experimental preparation with $pH_i > 7.7$. The only stable element is repetitive AP firing, i.e., the limit cycle (Fig. 7*B*). Increasing T to 9°C confers bistability to the model (Fig. 11). The steady-state current-voltage relation (Fig. 6A) is independent of T. However, V_0 is stabilized by the increase of T from 5 to 9°C. A 1-msec current pulse of relatively small amplitude elicited a subthreshold oscillatory response that relaxed back to V_0, similar to the result in Fig. 5*B*. A plot of this waveform in current-voltage space is also shown (Fig. 11*A*, top panel). A relatively large-amplitude current pulse elicited spontaneous repetitive firing (Fig. 10*D*), which clearly demonstrates bistability in the model for $T = 9$°C. As Guttman et al. (1980) noted, an unstable limit cycle must also exist under these conditions, i.e., a boundary between a region of attraction of the stable resting state, V_0, and a region of attraction for the limit cycle (Fig. 11*B* and *C*). This feature was demonstrated with current pulses in the vicinity of threshold for repetitive firing. When the pulse amplitude was adjusted to 1 part in 10^{10} near this threshold, large-amplitude, subthreshold oscillations were obtained lasting ~200 msec before relaxing back to V_0 (Fig. 11 *legend*). A small increase in pulse amplitude gave the result in Fig. 11*C*—a long train of oscillations that ultimately led to limit cycle activity. A plot of these results in current-voltage space reveals the quasi-stable limit cycle, which ultimately spirals down to V_0 (Fig. 11*B*), or spirals outward to the limit cycle (Fig. 11*C*). Large-amplitude subthreshold oscillations similar to the ones illustrated in Fig. 11 were occasionally observed in these experiments for $13 < T < 23$°C, although a long train of oscillations was not seen, probably because various noise sources in the experimental preparation do not allow the membrane potential to be adjusted as precisely as it was in the simulations.

A change from a monostable system (limit cycle) to a bistable one (limit cycle and stable equilibrium point) following an increase in temperature is consistent with the experiments, although the temperature range of this transition does not match the experiment. Another feature of the experimental results is the loss of spontaneous, repetitive activity above 23°C (Figs. 1–3). A similar effect occurs in the model for $T > 12$°C (Fig. 12). Superimposed records at 23 and 26°C (experiment) and 9 and 12°C (model) suggest a mechanism for this result. The preparation in Fig. 12*A* was bistable at 23°C. It was initially in its resting state. Spontaneous repetitive firing was produced by a 1-msec depolarizing current pulse. At 26°C, the rest state was the only stable element of the axon. An AP elicited by a 1-msec current pulse for this condition is shown superimposed upon the first AP of the train elicited by a current pulse at 23°C (Fig. 12*A*). The membrane potential following the AP at 26°C recovered (depolarized) toward V_0 at a faster rate than it did at 23°C, probably because I_K deactivation was faster, thereby allowing the background current (I_{NaP+} I_{Cl}) to depolarize the membrane potential to the vicinity of V_0 before recovery of I_{Na} inactivation was as complete as it was at 23°C. Consequently, the amplitude of available I_{Na} as the membrane potential reached V_0 was insufficient to elicit a second AP at the higher temperature. A similar mechanism underlies the corresponding result in the model (Fig. 12*B*).

Discussion

Ionic Mechanism of Spontaneous Firing

The key ionic current components underlying spontaneous firing in squid giant axons with alkaline pH_i

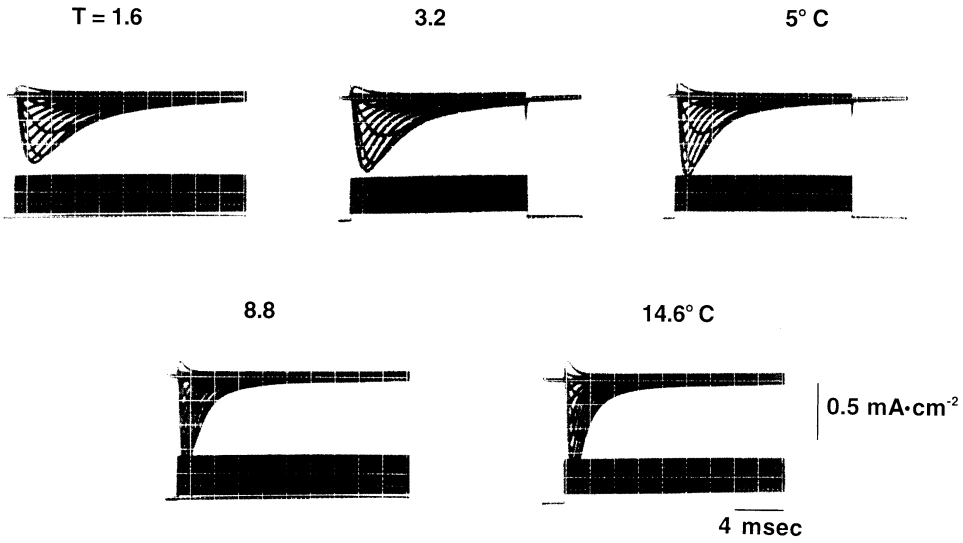

Fig. 9. Temperature dependence of I_{Na}. Each panel contains superimposed recordings from an axon perfused with 300 mM Cs^+ to block I_K and with voltage steps to −70, −60,..., +80 mV. A 2-sec rest interval was used between each step. Holding potential was −90 mV.

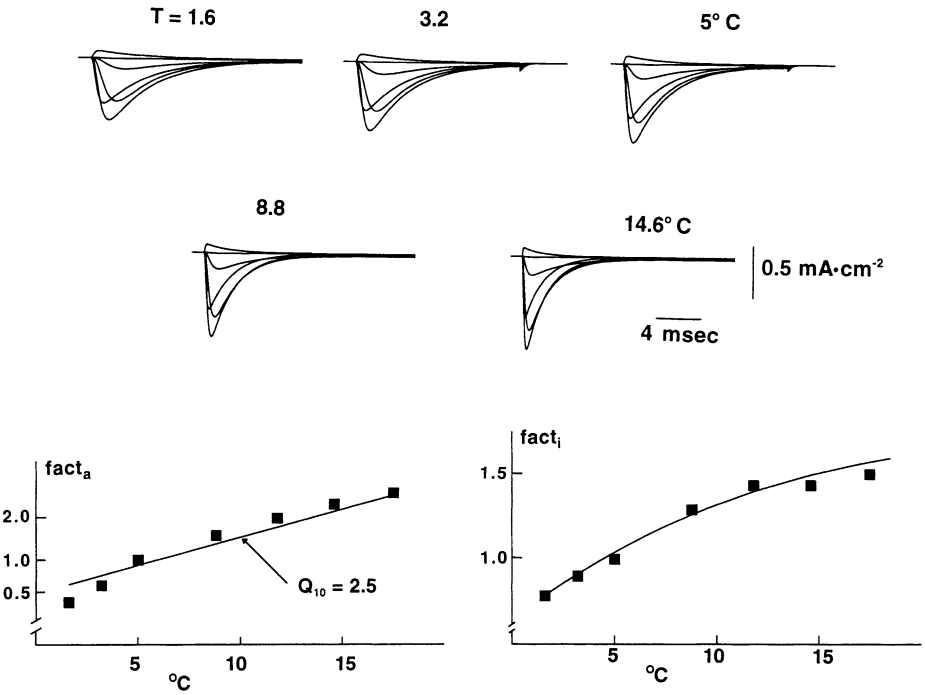

Fig. 10. Simulations of I_{Na} with the Vandenberg and Bezanilla (1991) model (Appendix) with voltage steps in each panel to −60, −40, −20, 0, +20, and +80 mV. Holding potential was −90 mV. The temperature dependence of the model was assigned to the activation (and deactivation) rate parameters and to the inactivation parameters as described in the text. The Q_{10} for activation was 2.5 (bottom left panel). The Q_{10} for inactivation appeared to saturate for $T \sim 15$°C. This effect was modeled by $2(3^{(T-5)/10}/(1+3^{(T-5)/10})$, which is represented by the theoretical curve in the bottom right panel.

are the persistent sodium ion current, I_{NaP}, and the leak component, I_L. The latter appears to be activated by intracellular protons since it is eliminated with pH_i above 7.7, thereby allowing the negative slope character of I_{NaP} to destabilize the equilibrium potential for $T < 13$°C. That is, a *loss* of a net inward current at subthreshold potentials leads to spontaneous activity. Spontaneous firing also occurs for $13 < T < 23$°C, although the equilibrium point is stable in this temperature range. That is, the axon is bistable. The role of I_{NaP} in squid axon electrical behavior for physiological pH_i is unclear, as is the role, if any, of the pH sensitivity of I_L. The latter, together with I_{NaP} and I_{Cl} depolarize the membrane potential to V_0 following an

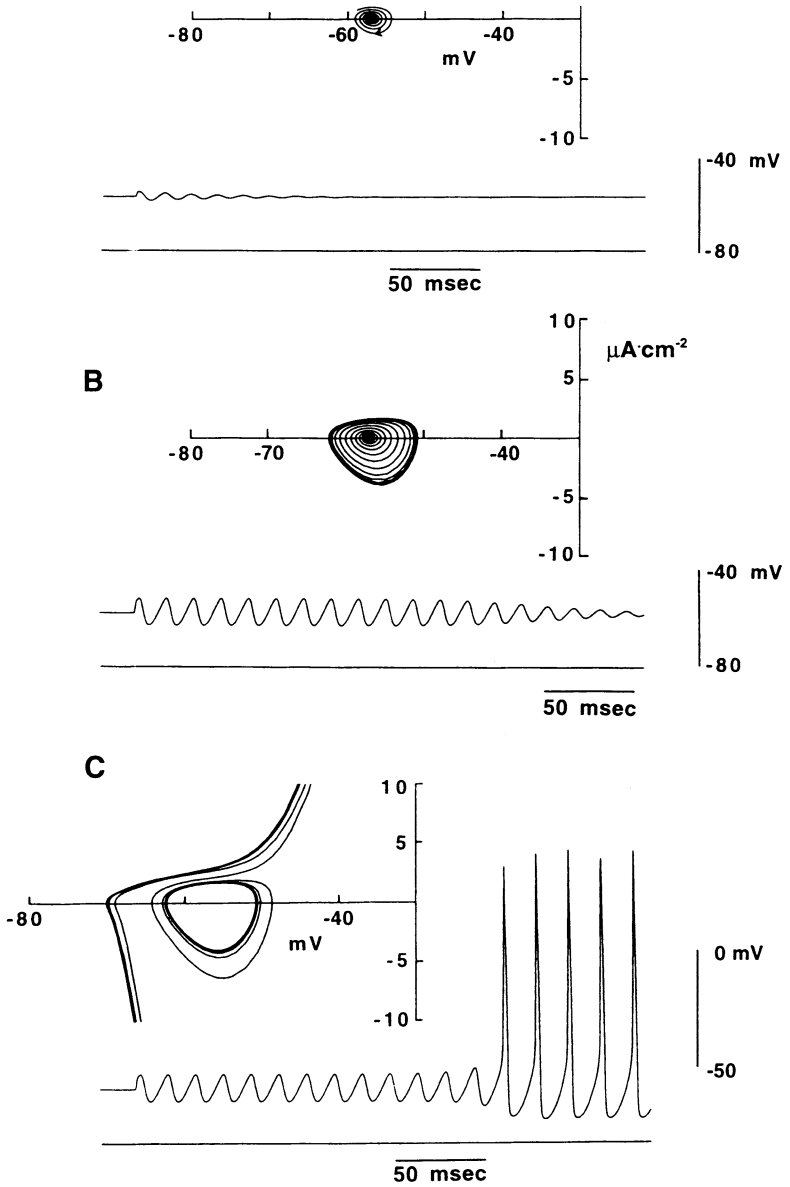

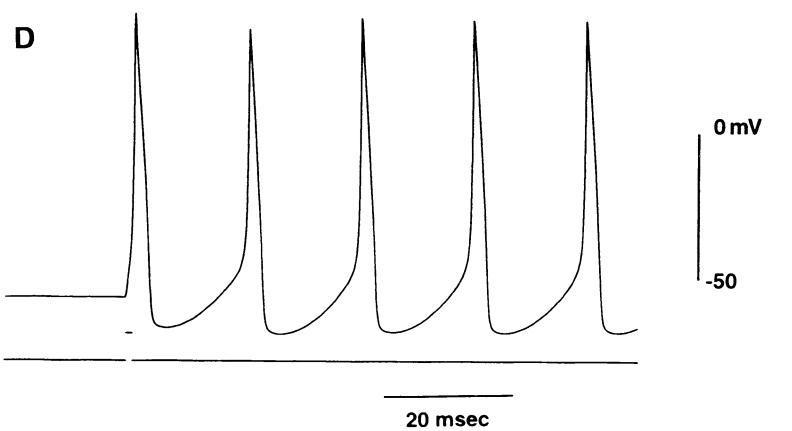

Fig. 11. Bistability in the model for $T = 9°C$. (*A*) The model was initialized at the resting level, V_0, which is stable for $T = 9°C$. A small-amplitude current pulse elicited a relatively small depolarization that relaxed back to V_0 in an oscillatory manner, as indicated also by the current-voltage plot above the response. (*B* and *C*) Response of the model to a 1-msec duration current pulse with amplitude given by -4.854100094 and -4.854100095 μA cm^{-2}, respectively. These results illustrate an unstable limit cycle—the border between the region of attraction of V_0 and the limit cycle corresponding to the Aps. (*D*) Response of the model to a relatively large-amplitude current pulse. This result demonstrates bistability.

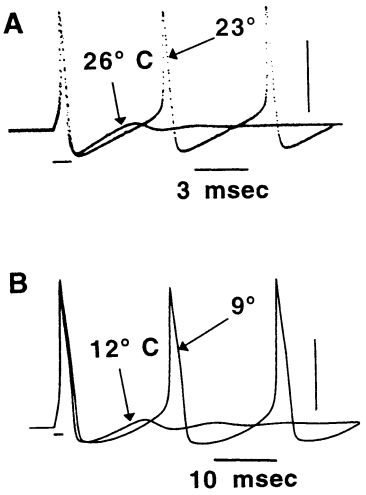

Fig. 12. Transition from bistability to quiescence with increasing temperature. (*A*) Comparison of electrical activity at 23 and 26°C. This preparation was bistable at 23°C. A depolarizing current pulse produced a transition between V_0 and the limit cycle. At 26°C the preparation was quiescent. An action potential elicited by a depolarizing current pulse is superimposed upon the recording at 23°C. The recovery from the foot of the AP was faster at 26 as compared to 23°C (arrow in *A*). The implications of this result are discussed in the text. (*B*) Simulations of a similar effect in the model for 9 and 12°C.

action potential and, together with I_{Na} and I_K, help to determine the resting potential. Moreover, the presence of I_L at pH_i 7.3 stabilizes the resting potential. The spontaneous firing reported here probably does not play a role in squid behavior since it is unlikely that pH_i remains above 7.7 for extended periods of time in vivo (Clay & Shrier, 2001).

Ion Currents in Other Neurons

The classical I_{Na} and I_K components that are present in most nerve cells of most animal species were reported first in the squid giant axon by Hodgkin and Huxley (1952). The persistent sodium ion current, I_{NaP}, which appears to be a channel distinct from I_{Na}, was first observed in mammalian brain slice preparations (Crill, 1996). It is a general feature of rhythmic activity in various brain regions (Crill, 1996; Agrawal, et al., 2001), and is also the critical subthreshold element of spontaneous firing in squid axons with alkaline pH_i. The I_L, or "leak" conductance was originally proposed by Hodgkin and Huxley (1952) to comprise all nongated components, including the chloride conductance. The latter has since been shown to have its own pathway (Inoue, 1985). The I_L terminology used here refers to a nonspecific, sustained, cation channel that passes both sodium and potassium ions. The novel feature of this channel is that it appears to be activated by intracellular protons (Clay & Shrier, 2001). A similar channel has been found in sensory neurons of dorsal root ganglia (Bevan & Yeats, 1991; Waldmann, et al., 1997), and has been termed the acid-sensing ion channel, or ASIC. All ASICs reported to date are activated by extracellular protons. The squid I_L channel differs in that it is activated by intracellular protons.

Bistability in Other Preparations

The type of bistability reported here, quiescence coexisting with spontaneous firing, is relatively rare. Another type of bistability—also uncommon—is the existence of two stable resting states. For example, Gadsby and Cranefield (1977) found two resting levels in cardiac Purkinje fibers for certain ionic conditions, as did Gallin (1981) in macrophages cultured from mouse spleen, and Barnes and Deschenes (1992) in cone photoreceptors. These results are attributable to an N-shaped current-voltage relation that crosses the voltage axis at three points, two of which are stable. The squid giant axon with alkaline pH_i has only a single equilibrium point with a stable limit cycle that encloses the equilibrium point in a current-voltage plot. An additional type of bistability, or even multistability, has been proposed by Canavier et al. (1994) for bursting neurons in molluscs. They suggest that two or more patterns of spontaneous firing may coexist for a given set of experimental conditions and that neuromodulators may provide the switch between these different behaviors.

One of the most dramatic forms of bistability is ventricular fibrillation and the conversion back to normal sinus rhythm either by electrical defibrillation or drug intervention (Lown et al., 1967). Another example in which quiescence is potentially life-threatening is sporadic apnea in sleeping infants (Southall & Talbert, 1988). This condition may be due to random switching of the central breathing oscillator from its normal rhythm (eupnea) to quiescence (apnea), i.e., bistability (Paydarfar & Buerkel, 1997). A less dramatic, but no less important example of bistability may occur during epileptic seizures (Durand and Bikson, 2001).

Conclusion

This report demonstrates temperature dependence of bistability in squid giant axons with alkaline intracellular pH_i. The preparation may provide a model for studies on rhythmicity in neurons. For example, we have recently used this system to demonstrate noise-induced transitions between the two stable states (Paydarfar, Forger & Clay, 2001). These results may have relevance concerning the role of noise in neuronal signaling.

The authors gratefully acknowledge discussions concerning these experiments with D. Forger and D. Paydarfar. The work was supported in part by the Canadian Institutes for Health Research (A.S.).

Appendix

Electrical activity was simulated using

$$C dv/dt + (I_{Na} + I_K + I_{NaP} + I_{Cl} + I_L) = 0, \quad \text{(A1)}$$

where C is membrane capacitance (1μF cm^{-2}), V is membrane potential in mV, t is time in msec, and the various ion current components are in units of μF cm^{-2}. The I_{Na} model is taken from Vandenberg and Bezanilla (1991) and is described by the kinetic diagram given above (Results) and in previous work from this laboratory (Clay, 1998). The I_{Na} amplitude is given by

$$g_{Na} P_0 V\{\exp[(V - E_{Na})/24] - 1\}/ \{[\exp(V/24) - 1][1 + 0.4\exp(-0.038\ V/24)]\}$$

where g_{Na} = 215 mScm^{-2}, E_{Na} = 64 mV, and P_0 is the probability that the channel is in the open state in the kinetic diagram.The vairious rate constants in the diagram (in msec^{-1}) are a = 7.55 exp[0.017(V−10)] ϕ_a, b = 5.6 exp[−0.00017(V−10)] ϕ_a, c = 21 exp[0.06(V−10)] ϕ_a, d = 1 .8 exp[−0.02(V−10)] ϕ_a, f = 0.56 exp[0.0004(V−10)] ϕ_a, g = exp[0.00004(V−10)], i = 0.0052 exp[−0.038(V−10)] ϕ_i, j = 0.00928 exp[−0.038(V−10)], y = 22 exp[(0.014 (V−10)] ϕ_a, and z = 1.26 exp[−0.048(V−10)] ϕ_a, where $\phi_a = 2.5^{(T-5)/10}$ and $\phi_i = 2[3^{(T-5)/10}/(1+3^{(T-5)/10})]$. The I_K component is given by $g_K\ n(V,\ t)^4\ V[\exp(V/24)\ -K_s(t)/K_I][\exp(V/24)\ -1]$, where g_K = 50 mS cm^{-2} and $n(V,t)$ is given by $dn/dt = -(\alpha + \beta)\ n + \alpha$, where $\alpha = -0.01(V+48)/\{\exp[-0.1\ (V+48)]\ -1\}\ \phi_n$, β = 0.1 exp[− (V+58)/25] ϕ_n, and $\phi_n = 3.63^{(T-5)/10}$. The intracellular K ion concentration, K_I, is 300 mM, and the K ion concentration in the extracellular space between the axonal membrane and the glial cells that surround the axon is given by $K_s(t)$, where

$$dK_s/dt = .007I_K - (K_s(t) - 10/(0.2 \times ((1 + (K_s(t) - 10)/2)^3)) - (K_s(t)/12. \quad \text{(A2)}$$

The I_{Cl} model is based on results in Inoue (1985) and is given by

$$I_{Cl} = 0.6V[\exp(V/24) - 0.02]/[\exp(V/24) - 1]. \quad \text{(A3)}$$

The I_{NaP} is given by (Rakowski et al, 1985; Clay Shrier, 2001)

$$I_{NaP} = 6(V/24)(0.03\exp(V/24) - 0.43)/ \times [(\exp(V/24) - 1)(1 + \exp(-(V + 65)/7))] \quad \text{(A4)}$$

The I_L component is given by 0.3 (V+49) for normal pH_i and 0 for alkaline pH_i (pHi > 7.7).

References

Agrawal, N., Hamam, B.N., Magistretti, J., Alonso, A., Ragsdale, D.S. 2001. Persistent sodium channel activity mediates subthreshold membrane potential oscillations and low-threshold spikes in rat entorhinal cortex layer V neurons. *Neuroscience* **102:**53–64.

Barnes, S., Deschenes, M.C. 1992. Contribution of Ca and Ca-activated Cl channels to regenerative depolarization and membrane bistability of cone photoreceptors. *J. Neurophysiol.* **68:**245–255

Bevan, S., Yeats, J. 1991. Protons activate a cation conductance in a sub-population of rat dorsal root ganglion neurons *J. Physiol.* **433:**145–161

Canavier, C.C., Baxter, D.A., Clark, J.W., Byrne, J.H. 1994. Multiple modes of activity in a model neuron suggest a novel mechanism for the effects of neuromodulators. *J. Neurophysiol.* **72:**872–882

Chiu, S.Y., Mrose, H.E., Ritchie, J.M. 1979. Anomalous temperature dependence of the sodium conductance in rabbit nerve compared with frog nerve. *Nature* **279:**327–328

Clay, J.R. 1998. Excitability of the squid giant axon revisited. *J. Neurophysiol.* **80:**903–913

Clay, J.R., Shlesinger, M.F. 1983. Effects of external cesium and rubidium on outward potassium currents in squid axons. *Biophys. J.* **42:**43–53

Clay, J.R., Shrier, A. 2001. Action potentials occur spontaneously in squid giant axons with moderately alkaline intracellular pH. *Biol. Bull.* **201:**186–192

Crill, W. 1996. Persistent sodium current in mammalian central neurons. *Ann. Rev. Physiol.* **58:**349–362

Durand, D.M., Bikson, M. 2001. Suppression and control of epileptiform activity by electrical stimulation: A review. *Proc. IEEE.* **89:**1065–1082

Frankenhauser, B., Moore, L.E. 1963. The effect of temperature on the sodium and potassium permeability changes in myelinated nerve fibers of *Xenopus laeyis*. *J. Physiol.* **169:**431–437

Gadsby, D.C., Cranefield, P.P. 1977. Two levels of resting potential in cardiac Purkinje fibers. *J. Gen. Physiol.* **70:**725–746

Gallin, E.K. 1981. Voltage clamp studies in macrophages from mouse spleen cultures. *Science* **214:**458–460

Guttman, R., Lewis, S., Rinzel, J. 1980. Control of repetitive firing in squid axon membrane as a model for a neuron oscillator. *J. Physiol.* **305:**377–395

Hodgkin, A.L., Huxley, A.F. 1952. A quantitative description of membrane conductance and its application to conduction and excitation in nerve. *J. Physiol.* **117:**500–544

Inoue, I. 1985. Voltage-dependent chloride conductance of the squid axon membrane and its blockade by some disulfonic stilbene derivatives. *J. Gen. Physiol.* **85:**519–537

Jalife, J. Antzelevitch, C. 1979. Phase resetting and annihilation of pacemaker activity in cardiac tissue. *Science* **206:**695–697

Kimura, J.E., Meves, H. 1979. The effect of temperature on the asymmetrical charge movement in squid giant axons. *J. Physiol.* **289:**479–500

Lown, B., Fakhro, A.M., Hood, W.B., Thorn, G.W. 1976. Coronary care unit – New perspectives and directions. *J. Am. Med. Assoc.* **199:**188–198

Matteson, D.R., Armstrong, C.M. 1982. Evidence for a population of sleepy sodium channels in squid axons at low temperature. *J. Gen. Physiol.* **79:**739–758

Otis, T.S., Gilly, W.F. 1990. Jet-propelled escape in the squid *Loligo opalescens*: concerted control by giant and non-giant motor axon pathways. *Proc. Natl. Acad. Sci. USA* 87:2911–2915

Paydarfar, D., Buerkel, D.M. 1997. Sporadic apnea—paradoxical transformation to eupnea by perturbations that inhibit inspiration. *Med. Hypoth.* **49:**19–26

Paydarfar, D., Forger, D.B, Clay, J.R., 2001. Control of transitions between repetitive firing and quiescence by stochastic stimulation of squid axons with membrane bistability. *J. Physiol.* **536:**120p

Rakowski, R., DeWeer, P., Gadsby, D. 1985. Threshold channels can account for steady-state TTX-sensitive sodium current of squid axon. *Biophys. J.* **47:**A31

Shrier, A., Clay, J.R., Brochu, R.M. 1990. Effects of tetrodotoxin on heart cell aggregates. *Biophys. J.* **58:**623–629

Southall, D.P., Talbert, D.G. 1988. Mechanisms for abnormal apnea of possible relevance to the sudden infant death syndrome. *Ann. NY Acad.* **533:**329–349

Vandenberg, C.A., Bezanilla, F. 1991. A sodium channel gating model based on single channel, macroscopic ionic, and gating currents in the squid giant axon. *Biophys. J.* **60:**1511–1533

Waldmann, R., Champigny, G., Bassilianna, F., Heurteaux, C., Ladzunski, M. 1997. A proton-gated cation channel involved in acid-sensing. *Nature* **386:**173–177

Winfree, A.T. 1977. Phase control of neural pacemakers. *Science* **197:**761–763

Wolfram, S. 1999. The Mathematica Book. 4th ed. Wolfram Media/Cambridge University Press, New York.